

Nanocrystallization kinetics of amorphous soft magnetic Fe₈₄Nb₇B₉ alloy

WeiLu^{(1)*}, Yuxin Wang⁽¹⁾ and Biao Yan⁽¹⁾

(1) School of Materials Science and Engineering, Shanghai Key Lab. of D&A for Metal-Functional Materials, Tongji University, Shanghai 200092, China

* Corresponding author.

Abstract –The primary nanocrystallization kinetics of amorphous Fe₈₄Nb₇B₉ alloy has been analyzed by non-isothermal DSC measurements. The local activation energies $E(\alpha)$ were also analyzed and its average value was about 468.7 kJ/mol. It was found that the primary nanocrystallization kinetics of amorphous Fe₈₄Nb₇B₉ alloy cannot be described successfully by JMA model while the two-parameter Sestak-Bergggren equation seems to be more appropriate in this case. The local activation energies and local Avrami exponent are introduced and they are applicable and correct in describing the primary crystallization process of the amorphous Fe₈₄Nb₇B₉ alloy according to the theoretical DSC curve simulation.

Soft magnetic alloys consisting of nanoscale bcc Fe grains have been developed by primary crystallization of melt-spun amorphous alloys, as typically exemplified in Fe–Si–B–Nb–Cu (Finemet) and Fe–M–B (M=Zr, Hf, Nb) (Nanoperm) systems. Among these nanocrystalline alloys, the Fe–M–B (M=Zr, Hf, Nb) alloys, such as Fe₉₀Zr₇B₃, Fe₈₄Nb₇B₉ and Fe₈₉Hf₇B₄, are particularly attractive because of the simplicity of the alloy system as well as their high saturation magnetization. Various research literatures reveal that the properties of nanocrystalline materials are closely related to their composition and the thermal treatment they experienced. The related studies are still carried out widely. But in these studies, most of them are reported on nanocrystallization in Fe–Zr–B and Fe–Zr–B–Cu alloys, little is known about the crystallization behavior especially the crystallization kinetics in M=Nb or Hf alloys. The aim of this presentation is to give a detailed investigation on the nanocrystallization kinetics of Fe₈₄Nb₇B₉ alloy considering the validity of Johnson-Mehl-Avrami (JMA) model, and to our knowledge, there are no previous results in the literature about the checking of the applicability of JMA model in Fe₈₄Nb₇B₉ alloy.

The amorphous ribbons of Fe₈₄Nb₇B₉ alloy were prepared by a single-roller melt spinning technique on a copper wheel in Ar atmosphere and the sample dimensions are 10mm wide and 20 mm thick. The complex primary crystallization kinetics of amorphous Fe₈₄Nb₇B₉ alloy was investigated with a NETZSCH-STA449C TG/DSC instrument using a continuous heating regime with heating rates β from 5 to 30°C/min. A N₂ gas flow was used for the ambient atmosphere. The temperature axis as well as the enthalpy axis was calibrated using indium and zinc standards for all the heating rates.

The local activation energy $E(\alpha)$ during the primary nanocrystallization of amorphous Fe₈₄Nb₇B₉ alloy was determined by an isoconversional method without assuming the kinetic model function. It was found that the local activation energy $E(\alpha)$ changed with crystalline fraction α and the average value was about 468.7 kJ/mol. The primary nanocrystallization kinetics of amorphous Fe₈₄Nb₇B₉ alloy cannot be described successfully by JMA model and the two-parameter Sestak-Bergggren equation seems to be more appropriate in this case. However, SB model has only a phenomenological value and gives no insight on the interpretation of the nanocrystallization mechanisms of Fe₈₄Nb₇B₉ alloy. The local activation energies and local Avrami exponent are introduced to describe the nanocrystallization mechanisms. The significant variation of local Avrami exponent and local activation energy with crystallized volume fraction demonstrates that the primary crystallization kinetics of amorphous Fe₈₄Nb₇B₉ alloy varies at different stages and the variable local activation energies $E_c(\alpha)$ and local Avrami exponents $n(\alpha)$ are applicable and correct in describing the primary crystallization process of the amorphous Fe₈₄Nb₇B₉ alloy according to the theoretical DSC curve simulation, as shown in Fig.1.

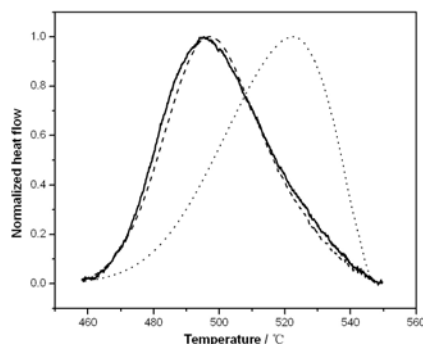


Figure 1: Theoretical and experimental DSC curves at heating rate of 5°C/min. Experimental curve (solid line); JMA theoretical curve using constant activation energy and Avrami exponent (dotted line); JMA theoretical curve using variable activation energies and Avrami exponents (dash line).